MetalMat

WILEY

MetalMat
ALL ABOUT METALS IN SCIENCE AND TECHNOLOGY Open Access

REVIEW OPEN ACCESS

Advancing the Solidification of Sn–Bi Alloys for Electronic Packaging: Challenges, Progress, and Future Directions

Marcella Gaute Cavalcante Xavier[1] | Bismarck Luiz Silva[2] | José Eduardo Spinelli[1]

[1]Department of Materials Engineering, Federal University of São Carlos, São Carlos, Sao Paulo, Brazil | [2]Department of Materials Engineering, Federal University of Rio Grande do Norte, UFRN, Natal, Rio Grando do Norte, Brazil

Correspondence: José Eduardo Spinelli (spinelli@ufscar.br)

Received: 18 June 2025 | **Revised:** 28 July 2025 | **Accepted:** 11 August 2025

Funding: The authors are grateful to CNPq—National Council for Scientific and Technological Development, Brazil and to FAPESP—São Paulo Research Foundation, Brazil (grant number #2023/06107) for their financial support. This study was financed in part by the Coordenação de Aperfeiçoamento de Pessoal de Nível Superior—Brasil (CAPES)—Finance Code 001.

Keywords: low-temperature soldering (LTS) | mechanical properties | microstructure | Sn–Bi alloys | solidification | wettability

ABSTRACT

In the early 2000s, the soldering industry faced a major shift due to regulations restricting Pb usage. As a result, four main alloy systems emerged as alternatives: Sn–Bi, Sn–In, Sn–Cu, and Sn–Ag. However, for reasons not initially evident, higher melting point alloys were the first to be widely developed, most notably the Sn–Ag–Cu (SAC) alloys, which became the industry standard due to their balanced performance in reliability, mechanical strength, and process compatibility. Over the past decade, increasing emphasis has been placed on low-temperature soldering (LTS), requiring studies not only on defects such as warpage, interfacial pores, and joint strength but also on the fundamental melting and solidification behavior of these alloys. Sn–Bi alloys have emerged as a commercial alternative, particularly for consumer products such as clients and server computers, while maintaining compatibility with surface mount technology (SMT) technology for high-volume manufacturing. The thermal fatigue reliability of Sn–Bi is also well-recognized. This short review will provide an overview of various studies conducted on the solidification behavior of Sn–Bi based alloys. The solidification paths, eutectic formation, morphologies, and properties will be explored. Future research directions comprise microalloying insights to improve ductility, interaction between Sn–Bi solder balls and SAC (Sn–Ag–Cu) pastes to mitigate PCB warpage, and exploring advanced characterization techniques such as X-ray microtomography (XMT) and nanohardness testing. These developments are essential for optimizing LTS alloys and ensuring their reliability in next-generation electronic packaging.

1 | Introduction

Key studies led by Dick Coyle and collaborators at Bell Labs in the early 2000s and beyond [1, 2] and collaborative industrial consortia such as iNEMI—International Electronics Manufacturing Initiative have provided essential insights into the solidification behavior and thermal fatigue reliability of Pb-free solder alloys, particularly Sn–Ag–Cu (SAC) systems. These works examined microstructural evolution under nonequilibrium conditions, intermetallic formation, and the effects of microalloying elements such as Bi, Sb, and Ni [3–5]. Although these studies have been critical for the development of Ag-containing Pb-free alloys, particularly SAC systems, Sn–Bi alloys have not received comparable attention, especially concerning their solidification behavior and phase evolution. This lack of systematic investigation highlights a significant gap in specialized literature. The present review addresses this by focusing specifically on Sn–Bi–based systems, thereby complementing the extensive body of work on SAC alloys and contributing to a broader understanding of solidification

This is an open access article under the terms of the Creative Commons Attribution License, which permits use, distribution and reproduction in any medium, provided the original work is properly cited.

© 2025 The Author(s). *MetalMat* published by Wiley-VCH GmbH.

phenomena in alternative, low-cost low-temperature lead-free solders.

Choosing Sn–Bi (tin–bismuth) solder alloys over Sn–Cu (tin–copper), Sn–Ag (tin–silver), or SAC alloys can be justified based on considerations related to phase diagram behavior, melting temperature, and especially cost of raw materials. The Sn–Bi binary system exhibits a simple eutectic reaction at approximately 138°C for a composition of 42 wt.% Bi, making it one of the lowest melting point lead-free solder systems available [6]. In contrast, the eutectic point in the Sn–Ag system lies at 221°C (for approximately 3.5 wt.% Ag), and for Sn–Cu, it is approximately 227°C at approximately 0.7 wt.% Cu [7, 8]. Thus, Sn–Bi alloys are highly suitable for LTS, especially in applications involving thermally sensitive substrates such as plastics, LEDs, and organic-based circuit boards [9].

From a microstructural standpoint, Sn–Bi solidifies into a simple eutectic structure without the formation of intermetallic compounds (IMCs), comprising only β-Sn and Bi phases [10]. This is in contrast to Sn–Ag and Sn–Cu solder alloys, which form intermetallic compounds (IMCs) such as Ag_3Sn and Cu_6Sn_5, respectively. These IMCs can not only be beneficial for mechanical strength but also contribute to brittleness and are prone to excessive growth during thermal aging, potentially affecting long-term joint reliability [6, 11]. The absence of IMCs in Sn–Bi eutectic solder simplifies solidification behavior and reduces concerns over brittle fracture interfaces.

Another significant factor favoring Sn–Bi over Sn–Ag is economic viability. Bi is considerably cheaper than Ag, and the cost differential is substantial. As of mid-2024, Bi was priced at around US$ 10–15/kg, while Ag remained very expensive at US$ 700–800/kg or higher depending on purity and form [12, 13]. Sn itself was around US$ 25–30/kg, and Cu was slightly cheaper, around US$ 8–9/kg. Therefore, although Sn–Cu is also a low-cost alternative, it lacks the low melting point and ease of processing that Sn–Bi provides. In contrast, Sn–Ag–based solders, particularly Sn-3.5Ag and Sn-Ag-Cu (SAC) alloys like SAC305, are widely used for high-reliability applications (e.g., aerospace and automotive), but their high cost is a limiting factor for large-scale consumer electronics [14].

Furthermore, the low melting point of Sn–Bi solder contributes to energy savings during reflow soldering, reducing thermal stress on components and enhancing assembly process efficiency. In SMT (surface mount technology) soldering processes, for instance, Sn–Bi solders offer advantages such as reduced components and substrate warping, enabling the use of thinner and smaller components. Their lower reflow temperatures (typically 170°C–190°C) also lead to energy savings and enhanced design flexibility [15]. These features make Sn–Bi an attractive choice for low-cost electronics, flexible circuits, and medical devices where thermal exposure must be minimized [9, 15]. However, it is also important to note that Sn-Bi solders can exhibit brittle fracture behavior due to the Bi phase inherent brittleness and may require optimization of cooling rates and joint geometry [16, 17]. Advances on this requires studies on fundamental solidification behavior of these alloys, as the evolution of microstructure and defect formation during soldering is intrinsically governed by solidification dynamics, including nucleation, growth kinetics, and phase transformation.

Considering that soldering with Sn-Bi, Sn–Bi–X, and other Sn–based alloys involves solidification under moderate and variable cooling rates depending on the alloy composition and the process used, as well as being influenced by wettability, it becomes critically important to understand the solidification and microstructural coarsening behavior in each case. Alloys with ternary additions aimed at improving ductility and fatigue resistance (both closely linked to coarsening behavior and the dendritic microstructural length scale) show trends that stand in contrast to those observed in Sn–Ag and Sn–Cu solder alloys [18, 19].

The combination of low melting point, relatively simplified microstructure, and lower elemental cost makes Sn–Bi a compelling alternative to Sn–Cu and Sn–Ag solders, particularly in cost-sensitive and low-temperature applications. To keep pace with the demands of modern electronic products, packaging technologies are evolving toward greater density, functionality, and integration [20]. Solder joints, which serve as the electrical and mechanical connection between the chip and the substrate, play a critical role in determining the reliability of individual components and, in some cases, the entire system [20]. Commonly used lead-free solders, such as Sn-0.7Cu and Sn-3.5Ag, require soldering temperatures exceeding 200°C. These elevated temperatures pose risks to heat-sensitive packaging materials and components, which demand the use of materials with high thermal resistance [21]. As a result, growing interest has emerged in low melting point solders like Sn–Bi and Sn–In, which enable soldering at lower temperatures and help minimize thermal degradation of materials during assembly [7].

This short review aims to provide a comprehensive overview of solidification of Sn–Bi–based solder alloys, focusing on their relevance for LTS applications. The discussion will be organized into key sections such as the historical evolution of solder alloys; the solidification behavior and eutectic features of binary Sn–Bi alloys; solidification in multicomponent Sn–Bi–X alloy systems, including wettability; future perspectives and challenges, such as improving ductility through alloying; and applying advanced characterization techniques like X-ray microtomography (XMT) and nanohardness in a correlational approach. Together, these topics will provide a comprehensive view of the current state of knowledge in solidification and emerging opportunities for Sn–Bi alloys in advanced electronic packaging technologies.

2 | Scope of This Review

This review is primarily based on research carried out over the past 15 years by the M2PS group at Federal University of São Carlos (https://www.m2ps.ufscar.br), Brazil, and the GPS group at University of Campinas, Brazil, focusing on the development, characterization, and application of Sn–Bi alloys. In addition to these contributions, several relevant studies from the broader scientific community have been included to provide a comprehensive overview of key topics and emerging trends related to this alloy system. The review addresses the solidification behavior, microstructural evolution, wettability, mechanical

29401402, 0, Downloaded from https://onlinelibrary.wiley.com/doi/10.1002/metm.70015 by Capes, Wiley Online Library on [13/10/2025]. See the Terms and Conditions (https://onlinelibrary.wiley.com/terms-and-conditions) on Wiley Online Library for rules of use; OA articles are governed by the applicable Creative Commons License

performance, and technological applications of Sn–Bi and Sn–Bi–X alloys, aiming to support both academic research and industrial innovation in the field of the LTSs.

3 | Overview of the Evolution of Sn–Bi Solder Alloys

The use of soldering and brazing alloys dates to 4000 BC, and was important in the Metal Age, subdivided into the Copper Age, Bronze Age, and Iron Age until the so-called Silicon Age [22]. The use of Sn–Pb alloys in ancient cultures dates back to around 350 BC, when water pumps made of bronze were sealed with Sn–Pb alloys. The Romans used Sn–Pb alloys extensively in the construction of aqueducts and also in the seaming of Pb pipes. However, the use was greatly expanded during the Industrial Revolution. In the early 20th century, soldering processes were introduced in the electronics industry as a reliable method for connecting copper wires. More recently, these soldered joints have assumed dual functions, mechanical and electrical, challenging the mechanical, creep, and fatigue resistance of Sn–Pb alloys. Thus, the applications of soldering processes in microchips and printed circuit boards are continuous [10, 22].

In recent years, a growing trend has been observed in the manufacturing of electronic devices. Over the years, these devices have been presenting an increasingly shorter life cycle or usage cycle. The most widely used alloy for soldering electronic microcomponents was the Sn-36 or Sn-40 wt.%Pb alloy due to its low melting point (approximately 185°C), low cost, and good wetting level on substrates used in industry (Cu, Ni, Pt, and Invar) [10, 23, 24]. However, the use of lead has been extremely harmful to the environment and to human beings, and its damage is already well-known to the international community. In this context, guidelines for the reduction and even restriction of the use of lead in the electronics industry have been implemented [10, 25]. Within this panorama, alternative lead-free alloys have emerged, whose objective is to replace the traditional Sn–Pb alloy [26]. Several alloys have stood out as alternatives to replacing the Sn–Zn, Sn–Cu, Sn–Bi, and Sn–Ag systems. However, these alloys have transformation temperatures, whether eutectic, liquidus, or solidus, higher than the Sn-36 wt.%Pb alloy, which are considered medium melting temperature alloys [22], whose main temperatures and compositions related to the eutectic reaction can be seen in Figure 1. This behavior directly has impacted the manufacturing system already set up for Sn–Pb alloys, in addition to reducing the use of lead-free alloys for electronic components that operate at low temperatures (< 180°C), involving polymeric parts, for example.

In this context, Sn–Bi alloys are important alternatives to replace lead-containing alloys. There is a substantial history of using eutectic Sn–Bi alloys in electronic applications that require solderability at low temperatures (< 180°C). Some interesting applications using eutectic Sn–Bi have been reported as electrically conductive adhesives, flip–chip interconnects, and bonding of thin film structures [27, 28]. Sn–Bi alloys with Bi contents between 30% and 60% (in weight %) are interesting alternatives, as they include good mechanical strength, excellent

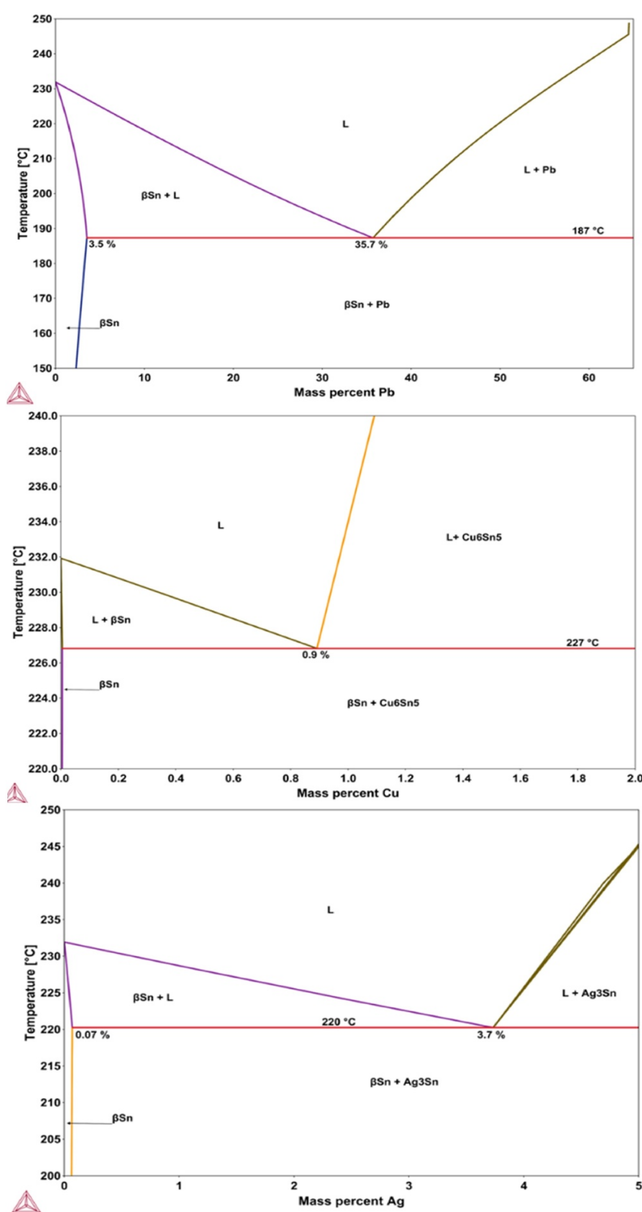

FIGURE 1 | Thermodynamic assessment via CALPHAD (TCSLD3 database, Stockholm, Sweden) of Sn–Pb, Sn–Cu, Sn–Ag, Sn–Zn, and Sn–Bi systems revealing partial phase diagram analysis, emphasizing Sn–Pb optimal melting temperature and higher processing temperatures of most Pb-free alloys, except for Sn–Bi (unpublished data).

creep resistance, low coefficient of thermal expansion, and low cost.

The solidification behavior of Sn–Bi alloys has been extensively studied and progressively refined since the late 1960s and early 1970s, when systematic investigations first began. A key point concerns the observation that the eutectic involves a highly efficient diffusive coupling process that can be faster than the isolated growth of a single phase, such as primary dendrites, even for alloys with pro-eutectic composition [29]. In this case, dendritic growth is restrained by the faster growth of the eutectic, and purely eutectic microconstituents are obtained. The temperature of the eutectic interface depends on the growth

29401402, 0, Downloaded from https://onlinelibrary.wiley.com/doi/10.1002/metm.70015 by Capes, Wiley Online Library on [13/10/2025]. See the Terms and Conditions (https://onlinelibrary.wiley.com/terms-and-conditions) on Wiley Online Library for rules of use; OA articles are governed by the applicable Creative Commons License

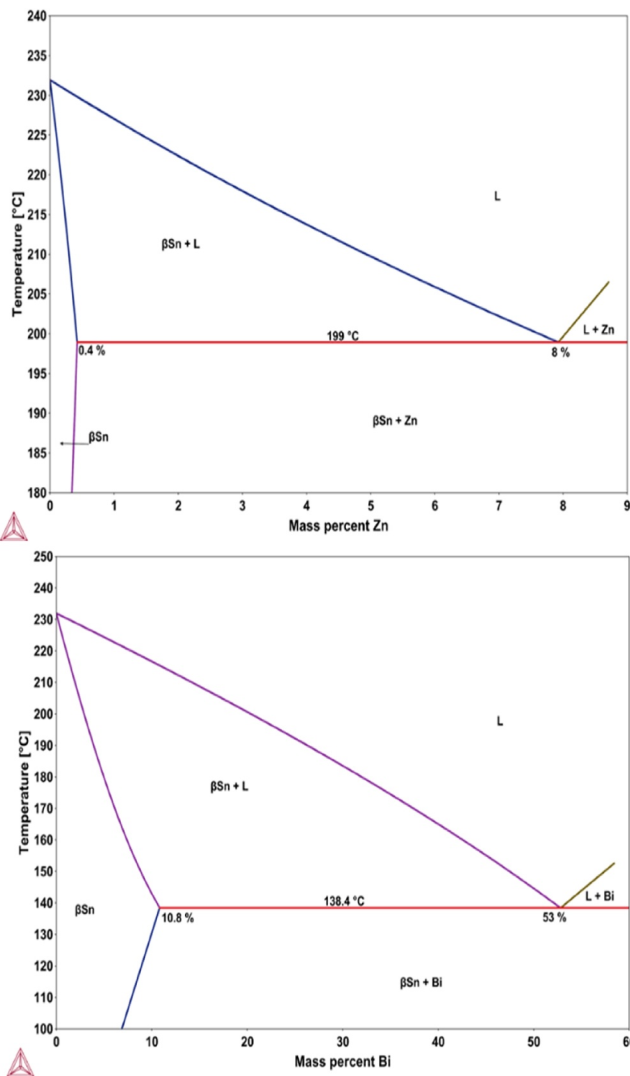

FIGURE 1 | (Continued)

rate, and this relationship is used together with the temperature of the dendrite tips of α and β crystals to define the so-called coupled growth zone, where the formation of completely eutectic microstructures occurs. Thus, the coupled growth region is a region dependent on the composition and the growth rate, in which the microstructure is completely eutectic. Outside this coupled growth zone, the microstructure will consist of primary dendrites with eutectic contained between their branches [29]. The coupled growth zone represents a set of temperatures and compositions, where the growth of the eutectic is faster than the growth of another primary phase, that is, within this region, the preference will be for the formation of this coupled eutectic [30].

The Sn–Bi system presents a coupled growth zone and is a nonfaceted–faceted eutectic, Sn–Bi, respectively [30, 31]. Gigliotti et al. [31] constructed a partial Sn–Bi phase diagram with an asymmetric coupled growth zone using Bi concentrations between 55% and 65% (in weight %) and two nucleation temperatures, 130° and 134°C. Furthermore, Sn–Bi alloys rich in Sn showed in their microstructures a predominance of irregular eutectic, whereas for alloys with high Bi content, the dominant eutectic is the complex regular eutectic (with two types of regions observed—(i) regular zones repeating and (ii) zones in random orientation) [32, 33].

In addition to insights into solidification mechanisms, extensive efforts have been directed toward technological developments. The development of Sn–Bi solder alloys has progressed through distinct phases, beginning with early patents in 2002 and 2007 focused on Sn–Bi–Pb systems and semiconductor bump applications. By 2014, Bi–Sn high-temperature variants were introduced to meet performance demands above 250°C. From 2016 onward, innovations emphasized alloy strengthening through additions such as Sb, Ce, Ti, Mn, and Cu, enhancing mechanical properties and tailoring melting behavior, as summarized in Table 1. The most recent advancement, represented by US11999018B2 (2024) [42], presents a comprehensive formulation scope for Sn–Bi and Sn–In systems, aligning with current commercial and industrial requirements.

4 | Solidification Behavior and Eutectic Features in Binary Sn–Bi

Shen et al. [43] and Zhu et al. [44] demonstrated that the Sn–Bi alloys perform low ductility due to the formation of brittle phases in the solder joints. Additionally, the strong tendency of Bi to segregate during solidification is recognized as a drawback of Sn–Bi alloys [45, 46]. At low Bi contents, Bi mainly interacts with tin to form small solid precipitates. However, as the Bi content increases, it begins to solidify into coarser eutectic phases, which causes a decline in the strength of the solder joints [47]. This occurs due to Bi segregation (accumulation) at the joint interface, leading to a slightly thicker IMC layer, as can be seen in Figure 2. Considering that both the Bi phase and the IMC layer in the solder joint are brittle, cracks occur more easily at the interface as the Bi content in the solder joint increases. These drawbacks related to segregation and coarse eutectic microconstituents are solidification-related issues. The following studies demonstrate some alternatives to better understand solidification and minimize these occurrences.

Silva et al. [48] performed experiments in order to directionally solidify a near-eutectic Sn–52 wt.% Bi alloy. It obtained a microstructure of Sn-rich dendrites and a eutectic mixture (Bi-rich and Sn-rich phases), with unevenly distributed Bi precipitates. To better characterize this complex eutectic morphology, as seen in Figure 2, the alloy was solidified under controlled conditions, revealing two distinct eutectic morphologies—fine island-like and fishbone-like structures, so called fine and coarse eutectic zones. These zones have been translated in terms of microstructural spacing. As can be seen in Figure 3, it was demonstrated that two experimental laws can describe the evolution of the eutectic spacing with the solidification velocity. The −1/2 exponent proposed by Jackson and Hunt was able to account for the unsteady-state growth of both eutectic scales, varying from 1.3 to 3.1 μm and from 0.8 to 1.8 μm. The differences between λ_{coarse} and λ_{fine} can be seen in Figure 3. This large variation over short distances within the Sn–Bi eutectic structure may affect the mechanical and electrical properties of the alloy.

29401402, 0, Downloaded from https://onlinelibrary.wiley.com/doi/10.1002/metm.70015 by Capes, Wiley Online Library on [13/10/2025]. See the Terms and Conditions (https://onlinelibrary.wiley.com/terms-and-conditions) on Wiley Online Library for rules of use; OA articles are governed by the applicable Creative Commons License

TABLE 1 | Progression of some Sn–Bi solder alloy patents over the years, covering Pb-containing systems (2002–2007), high-temperature applications (2014), and alloys with enhanced mechanical properties (2016–2024). Reference links are provided.

Year	Patent number	Highlights	Link
2002	US 4816219A	Low-temperature Sn–Bi–Pb alloy (< 150°C) with Ga/Ni for fusible solder.	https://patents.google.com/patent/US4816219A/en [34]
2007	US 20070152331A1	Sn–Bi family solder for semiconductor bumping with Cu/Zn/Ag additions.	https://patents.google.com/patent/US20070152331A1/en [35]
2015	US 9205513B2	High-temperature (≥ 250°C) Bi–Sn solder strengthened with Sb/Ag.	https://patents.google.com/patent/US9205513B2/en [36]
2016	WO 2018046763A1	Lead-free Sn–Bi with Mn/Sb/Cu for electronics assembly.	https://patents.google.com/patent/WO2018046763A1/en [37]
2016	US 11479835B2	Low-temp Sn–Bi–Sb–Ce/Ti alloys melting at 140°C–153°C.	https://patents.google.com/patent/US11479835B2/en [38]
2017	US 20170066089A1	High-reliability lead-free solder (Sn–Bi–Sb).	https://patents.google.com/patent/US20170066089A1/en [39]
2020	US 5411703A	High-solidus Sn with Sb/Bi/Cu (≈90% Sn) for strong joints.	https://patents.google.com/patent/US5411703A/en [40]
2022	EP 2739432B1	Sn–Bi eutectic (~138°C) with Cu/Co—high toughness and low aging.	https://data.epo.org/publication-server/rest/v1.0/publication-dates/20220105/patents/EP2739432NWB1/document.pdf [41]
2024	US 11999018B2	Broad Sn–Bi/In alloys (2%–60% Bi) with Ag, Cu, Sb, Zn, Ni, Co, etc., liquidus < 210°C.	https://patents.google.com/patent/US11999018B2/en [42]

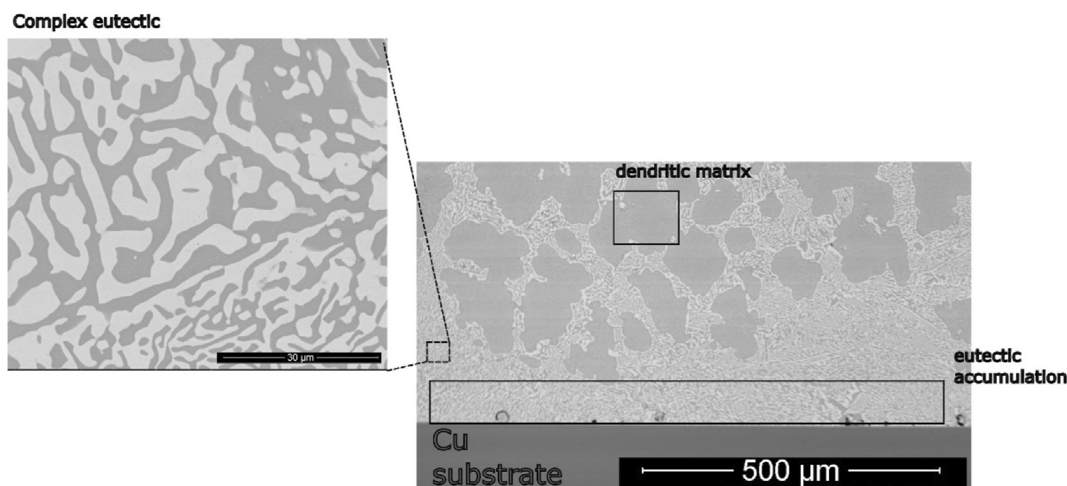

FIGURE 2 | SEM images of assembly connected by soldering at 200°C for 15 min between Sn-40 wt.% Bi alloy and copper. Details of the formed phases and constituents, highlighting the strong segregation (accumulation) of Bi at the bottom of the bulk alloy (unpublished images).

Solidification control can significantly influence the mechanical properties of solder alloys. One strengthening mechanism is related to the accumulation of dislocations at the interface between primary dendrites and the eutectic constituent. This dislocation buildup, often caused by shrinkage mismatch and lattice incompatibility during solidification, contributes to the overall hardening of the alloy. To a certain extent, the effectiveness of this mechanism can be correlated with the eutectic spacing, as suggested by Silva et al. and Osorio et al. [49, 50] in their studies with hypoeutectic Sn–Bi alloys.

As observed in Figure 4, for the Sn-34 and Sn-52 wt% Bi alloys, the yield tensile strength (σ_y) and elongation (δ) increased as the fine-scale eutectic spacing decreased. This refinement led to a more homogeneous distribution of Bi-rich and Sn-rich phases across the microstructure, which contributed positively to mechanical performance. In contrast, the Sn-58 wt% Bi eutectic alloy exhibited the lowest tensile properties, showing an opposite trend relative to the hypoeutectic compositions. This behavior was attributed to the predominance of eutectic structures in the Sn-58 wt% Bi alloy, including a high fraction of faceted Bi particles and trifoil-like morphologies, which are less effective in strengthening. The ductility of the Sn-52 wt% Bi alloy exhibits a strong dependence on the microstructural spacing. This highlights the critical role of solidification kinetics, Bi content, and eutectic spacing control in tailoring the mechanical properties of the alloy [49].

29401402, 0, Downloaded from https://onlinelibrary.wiley.com/doi/10.1002/mem.70015 by Capes, Wiley Online Library on [13/10/2025]. See the Terms and Conditions (https://onlinelibrary.wiley.com/terms-and-conditions) on Wiley Online Library for rules of use; OA articles are governed by the applicable Creative Commons License

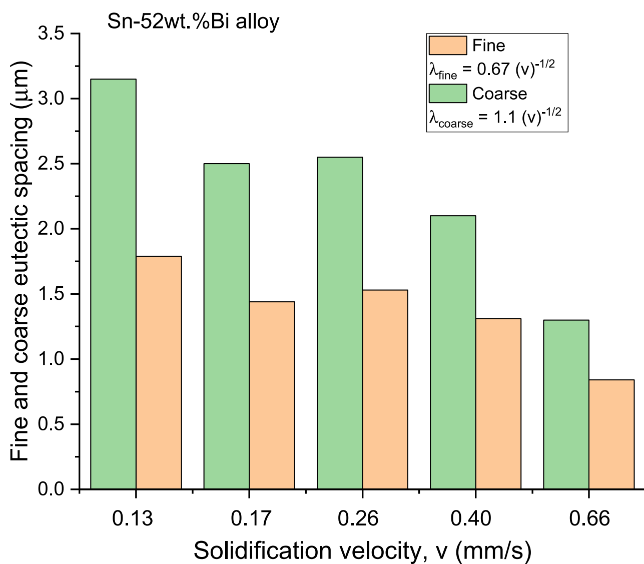

FIGURE 3 | Fine and coarse eutectic spacing and solidification velocity for directionally solidified Sn–52 wt.% Bi alloy [48]. At least 40 spacing measurements have been performed for each solidification velocity sample. The results are represented in average to facilitate comprehension. The maximum standard deviations for spacing attained 0.3 μm (Reproduced with permission from Elsevier. Elsevier Inc. License ID: 1629060-1).

Another important yet underexplored aspect in Sn–Bi alloys is coupled growth, already mentioned in the Section 3. For a given alloy system, the ability to form a wider or narrower range of eutectic microstructures can be assessed by mapping the solidification velocity alongside the resulting morphologies, which defines the so-called coupled zone. In the case of Sn–Bi alloys, the presence of complex regular structures may cause the microstructure to behave locally as nonfaceted/faceted (nf/f) eutectics. This justifies the coupled zone being more strongly biased toward the faceted Bi phase, as observed by Kakitani et al. [51]. Gigliotti et al. [31] also demonstrated a solidification diagram significantly skewed toward the Bi-rich side.

5 | Solidification Behavior in Multicomponent Sn–Bi–X

Although the study of binary Sn–Bi alloys is essential, the addition of third and even fourth elements is a fundamental strategy to enhance alloy quality and performance. Ternary or multicomponent alloys require greater care regarding chemical composition, segregation and nucleation, and growth of primary or intermetallic phases, among other metallurgical characteristics, which generally result in higher production costs. In the context of alternative Pb-free soldering alloys, the literature shows that several studies are focused on ternary or multicomponent alloys [10, 22]. The alloying elements added to binary Sn–Bi alloys are inserted with the purpose of improving specific properties, such as mechanical strength, wetting level, thermal fatigue, electrical conductivity, creep, and solderability. Among the many base alloys in several investigations, the following ternary systems deserve attention: Sn–Ag–Cu, Sn–Bi–Zn, Sn–Bi–Cu, and Sn–Bi–Ag. A focus will be given to these last two. The Sn–Bi–Ag and Sn–Bi–Cu alloys have high potential for applications in the electronics industry as substitutes for Pb-containing alloys.

The addition of a small amount of copper (Cu) (< 1.0 wt.%) to an Sn-based solder alloy can help prevent dissolution of the base metal. Furthermore, it is possible to achieve a fine and uniform dispersion of small Cu-containing precipitates to produce fine and homogeneous microstructures [52]. Silver (Ag), which has limited solubility in tin (Sn) [22], when added, aims to form intermetallic particles (mainly Ag_3Sn) with optimized properties and characteristics such as mechanical resistance, wettability in copper and nickel substrates, and more stable microstructure above room temperature [53–56]. As demonstrated by Ren and Collins [57], the addition of 0.4 wt.% Ag to Sn58Bi solder significantly enhances its mechanical properties, including tensile strength, yield strength, and Young's modulus, due to microstructural refinement and precipitation hardening. However, this improvement comes at the expense of ductility, attributed to the formation of brittle Ag_3Sn intermetallic compounds. The study also reports improved board-level reliability during thermal cycling, as Ag_3Sn particles inhibit microstructural coarsening by stabilizing Sn–Bi phase boundaries.

Silva et al. [58] reported the effect of Cu (0.1 and 0.7 wt.%) and Ag (2 wt.%) additions on the microstructure of the directionally solidified Sn-34 wt.%Bi binary alloy. The Sn–Bi–Cu and Sn–Bi–Ag alloys exhibited microstructures composed of Sn-rich dendrites with Bi precipitates inside, surrounded by complex ternary eutectic constituents formed by (Sn + Bi) and their respective intermetallic compounds, Cu_6Sn_5 and Ag_3Sn, respectively (Figure 5a–c). It is worth mentioning that these intermetallics have been observed both as primary particles and as eutectic phases. The authors also highlighted the presence of two eutectic scales (Figure 5d), a coarser and a finer one. Silva et al. [58] stated that the additions of Cu and Ag refined the secondary (λ_2) dendritic arms along the Sn–Bi–Cu and Sn–Bi–Ag castings. Cu and Ag have been consumed for the formation of the intermetallics Cu_6Sn_5 and Ag_3Sn, collaborating in the generation of ternary eutectics in isolation in the as-cast microstructures. The authors reported that the eutectics in the Sn–Bi–Cu and Sn–Bi–Ag alloys grew according to the classical Jackson and Hunt relationship [59] for the growth of lamellar eutectics, between microstructural coarsening and solidification rate.

Silva et al. [60, 61] investigated the influence of Cu (0.1 and 0.7 wt.%) and Ag (2 wt.%) additions on the tensile mechanical properties and fracture modes of directionally solidified nonequilibrium Sn-34 wt.% Bi–xCu and Sn-34 wt.% Bi–yAg alloys. Figure 5e and f shows the *stress* versus *strain* graphs and the respective fracture surfaces for the alloys examined, based on samples solidified under two distinct cooling rates, leading to varying degrees of dendritic coarsening. The behavior of high cooling rate samples approximately at 12.0°C/s and low cooling rate samples at 0.1°C/s can be seen in Figure 5e and f. The 0.1 wt.% Cu grade exhibited the best and most balanced mechanical behavior, that is, it achieved suitable strength and ductility. This ductility behavior was observed throughout the Sn-34 wt.% Bi-0.1 wt.% Cu casting and can be confirmed by the fracture surfaces, which indicated a ductile fracture mode with

29401402, 0, Downloaded from https://onlinelibrary.wiley.com/doi/10.1002/metm.70015 by Capes, Wiley Online Library on [13/10/2025]. See the Terms and Conditions (https://onlinelibrary.wiley.com/terms-and-conditions) on Wiley Online Library for rules of use; OA articles are governed by the applicable Creative Commons License

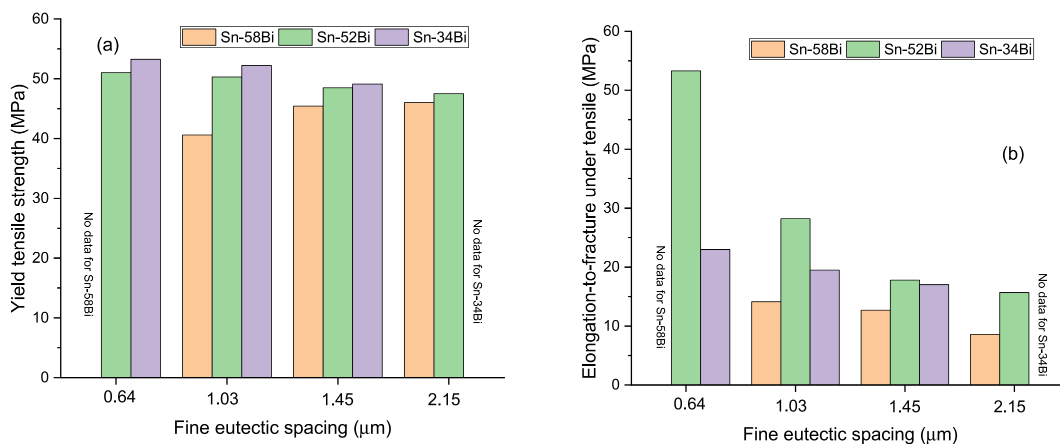

FIGURE 4 | Variation of (a) yield tensile strength and (b) elongation as a function of fine eutectic spacing for the Sn-34 wt.% Bi, Sn-52 wt.% Bi, and Sn-58 wt.% Bi alloys. Data represent the average values from triplicate tensile tests [49]. Deviations are smaller than 5% for each triplicate average (Reproduced with permission from Springer Nature. License ID: 1629060-2).

the presence of dimples. The 0.7 wt.% Cu and 2 wt.% Ag contents caused significant losses in both mechanical strength and elongation, exhibiting fracture surfaces with cleavage planes and dimples, or only cleavage planes. The alveolar fracture mode has been observed mainly for the high cooling rate samples because in this condition there is a more refined microstructure, both dendritic arrangements and Bi particles, due to the higher cooling rate values as shown in Figure 5e.

Thermal interface material (TIM) can be defined as any material applied between the interfaces of two components to improve thermal coupling between these devices, as an air gap is created at the coupling gap of these components [62–64]. Typically, TIM is used between a heat-generating device (microprocessor, photonic integrated circuits or chip) and a heat-dissipating device to remove heat from the component. TIM is necessary to maintain reliable operation and increase the service life of these components. TIMs can be of different materials and configurations such as thermal greases, phase change materials, gap filler pads, thermal tapes, thermal epoxies, gels, and solders [62–64]. An example of the latter is soldering alloys based on the Sn–Bi system with the addition of gallium (Ga). Da Silva et al. [65] analyzed the effects of adding 2 wt.% Ga at the interfaces between Sn-40 wt.% Bi–Ga and Sn-58 wt.% Bi–Ga binary alloys and copper substrate. Ga modified the growth morphology of the Sn-rich primary phase, from unfaceted to faceted. The Ga additions caused a deterioration in the tensile mechanical properties, with samples exhibiting zero or almost zero plastic deformation. In addition, Ga reduced the wettability of the Cu substrate because the Sn–Bi–Ga alloys exhibited higher contact angles and lower levels of areal scattering. The authors reported that the only positive point of the Ga addition was the suppression of intermetallic layers between the alloy/substrate containing Cu–Sn, which is detrimental to the soldered joint.

6 | Wettability

For a good metallurgical bond to occur, the two metals must interact effectively. This requires the liquid metal to flow properly over the solid surface during soldering. The term wettability is commonly used in the context of low melting point solder alloys and refers to a liquid ability to spread over a solid surface [66, 67]. This property is quantified by the contact angle (θ), formed where the liquid meets the solid. If θ is between 0° and 90°, the system exhibits interaction. If θ is between 90° and 180°, the system is considered nonwettable, indicating poor interaction. Despite its importance, the wettability of soft solder alloys is often overlooked. However, with the growing development of lead-free soldering technologies, interest in evaluating contact angles to assess system wettability has increased.

Wettability is crucial for the integrity of Sn–Bi solder joints, as poor spreading of the solder can lead to defects such as voids, cold joints, delamination, and irregular intermetallic formation. These issues compromise mechanical strength, electrical conductivity, and long-term reliability [68].

The study performed by Silva et al. [69] highlights the critical influence of wettability, quantified by the contact angle (θ), on the solidification behavior of Sn–Bi–based solder alloys. Through systematic wetting and directional solidification experiments, the authors demonstrate that lower contact angles (θ), especially in Sn–34Bi–0.1Cu (wt.%) alloys, correspond to better wettability and higher interfacial heat transfer, which directly increases the initial cooling rate ($\dot{T}$). In contrast, higher contact angles observed in other Sn–Bi–X alloys (e.g., with 2 wt.% Ag) indicate reduced wettability and lower $\dot{T}$. Since inadequate wettability can hinder solder spreading and solidification dynamics, this behavior is directly linked to the risk of forming interfacial defects such as voids, cold joints, and irregular intermetallic layers in Sn–Bi solder joints.

As demonstrated by Leal et al. [70], the addition of indium significantly improves the wettability of Sn–Bi solder alloys. The Sn-40% Bi-10% In alloy exhibited lower stabilized contact angles (24° on copper and 26° on nickel) than 45° and 53° for Sn-40% Bi, and 28° and 24° for Sn-50% Bi alloys, respectively. These results indicate that the presence of indium enhances spreading and wetting behavior. Although higher Bi content

29401402, 0, Downloaded from https://onlinelibrary.wiley.com/doi/10.1002/metm.70015 by Capes, Wiley Online Library on [13/10/2025]. See the Terms and Conditions (https://onlinelibrary.wiley.com/terms-and-conditions) on Wiley Online Library for rules of use; OA articles are governed by the applicable Creative Commons License

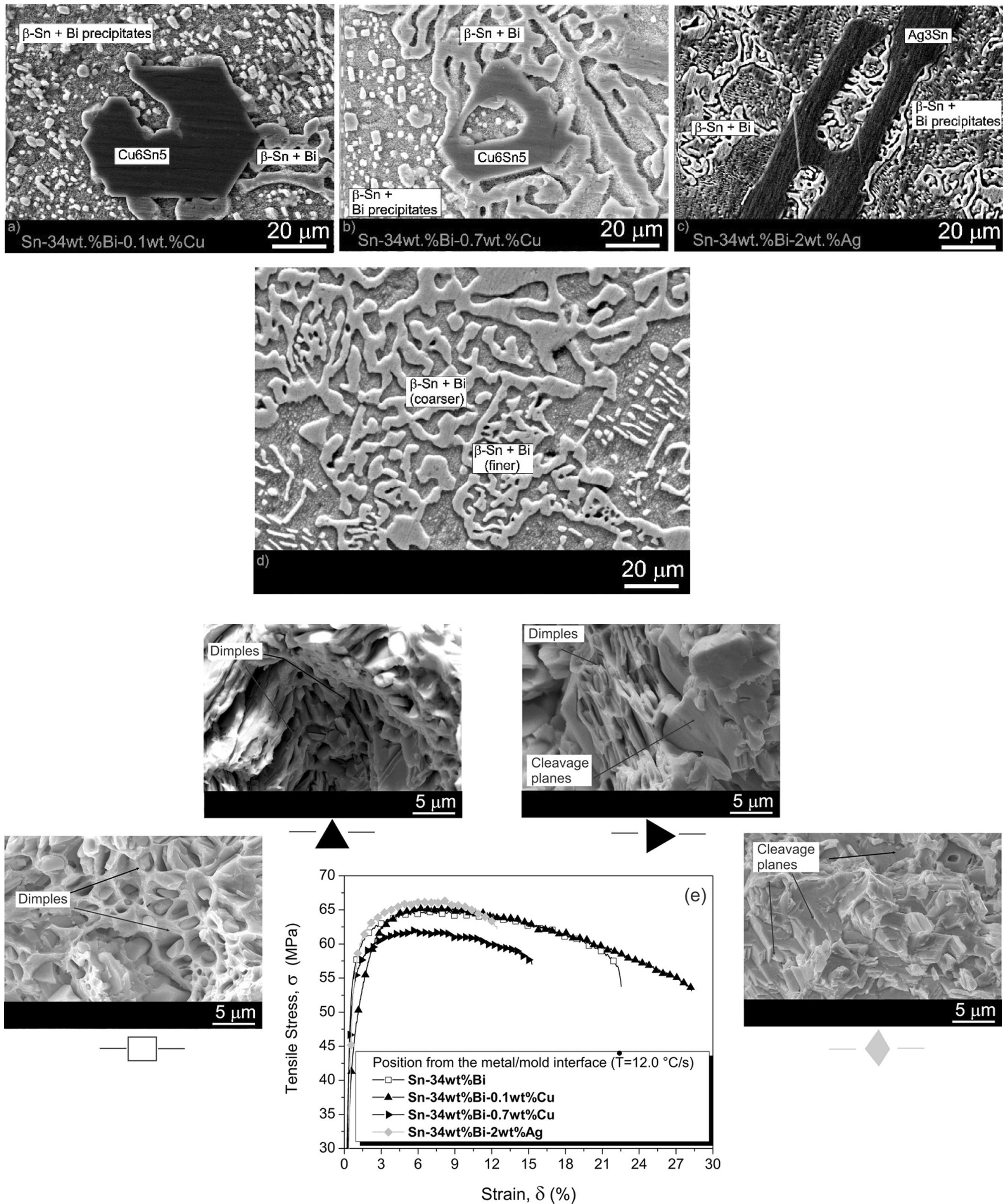

FIGURE 5 | SEM images of the as-cast microstructures for (a) Sn-34 wt.% Bi-0.1 wt.% Cu, (b) Sn-34 wt.% Bi-0.7 wt.% Cu, (c) Sn-34 wt.% Bi-2 wt.% Ag alloys, and (d) micromorphological contrast between the coarser and finer eutectic regions in the Sn–Bi alloy. Stress versus strain plots and respective fracture surfaces for Sn–Bi, Sn–Bi–Cu, and Sn–Bi–Ag, for (e) high cooling rate (~12.0°C/s) and (f) low cooling rate (~0.1°C/s) samples (unpublished data and images).

also contributes to improved fluidity due to a reduced melting point, it compromises ductility due to the brittle nature of the Bi phase. The findings align with those by Nabihah and Naralukmal [71], who reported that indium reduces surface tension, thereby decreasing the contact angle and enhancing wettability.

29401402, 0, Downloaded from https://onlinelibrary.wiley.com/doi/10.1002/metm.70015 by Capes, Wiley Online Library on [13/10/2025]. See the Terms and Conditions (https://onlinelibrary.wiley.com/terms-and-conditions) on Wiley Online Library for rules of use; OA articles are governed by the applicable Creative Commons License

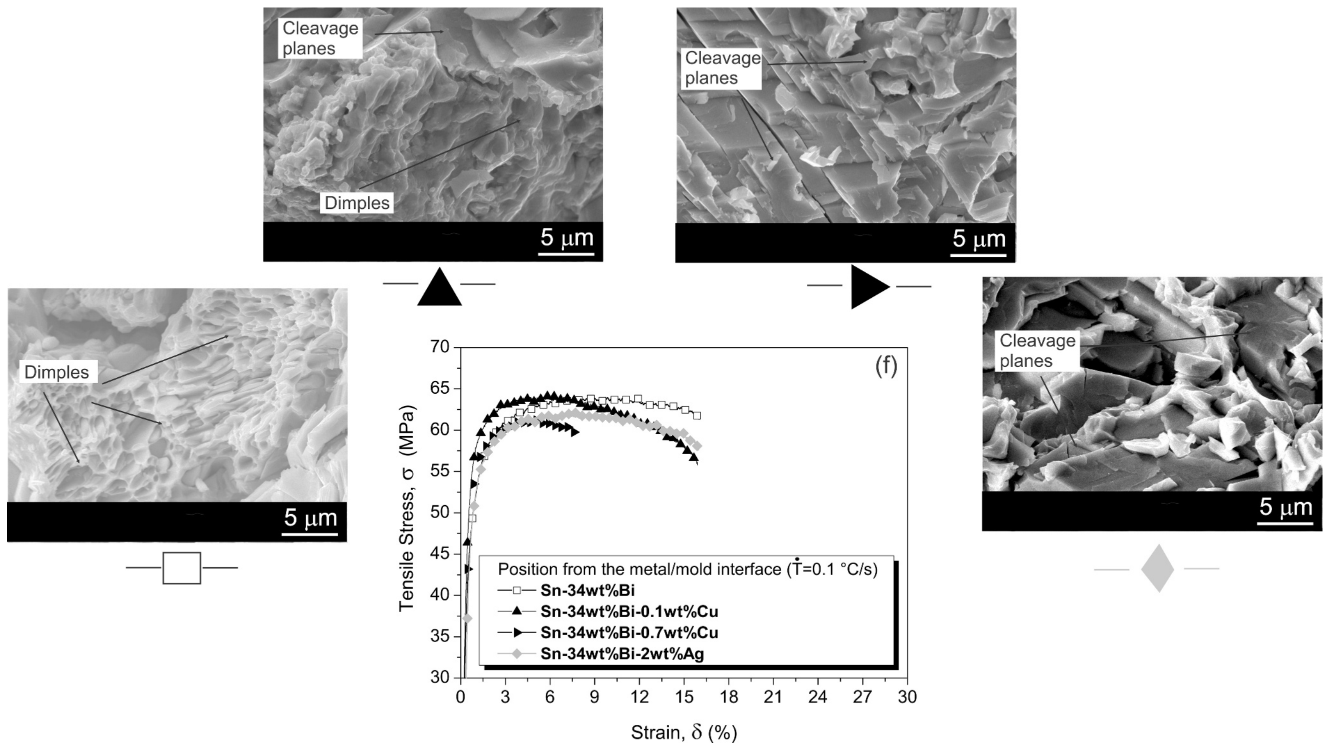

FIGURE 5 | (Continued)

7 | Conclusions

Among the points discussed, it becomes clear how important it is to understand the solidification process and its impact on the formation and morphology of phases in the Sn–Bi solder alloys. Equally important is the controlled addition of alloying elements to improve ductility. Solidification also plays a key role in wettability and in the solidification mode, which is influenced by the intimate contact between the solder and the substrate. This contact not only governs heat extraction but also affects the structural characteristics of the solder alloy. All these aspects are and will continue to be essential for the development of new applications and for improving the quality of processing and solder Sn–Bi joints.

8 | Future Perspectives and Challenges

Four key points deserve attention as future directions in this field: (i) mitigating printed circuit board (PCB) warpage, (ii) exploring advanced characterization techniques such as X-ray microtomography (XMT), (iii) assessing local properties through nanoindentation testing, and (iv) verifying microstructural stability envisaging new applications for Sn-Bi. Each of these points will be briefly commented on below.

i. Warpage, defined as the distortion or bending of substrates during soldering processes, especially during surface mount technology (SMT) reflow, becomes a critical issue in ultrathin electronic assemblies. It arises primarily from the mismatch in the coefficient of thermal expansion (CTE) between materials such as silicon dies, organic substrates, and copper layers, leading to compressive and tensile stresses during thermal cycling. This deformation can result in open joints, bridging, and loss of coplanarity, significantly affecting joint yield and reliability. Figure 6 shows the occurrence of head-on-pillow, open joint, and bridging defects induced by package warpage during reflow operations.
Studies have shown that up to 50% of assembly defects in thin packages are directly or indirectly related to warpage [72–74]. To mitigate this, a key strategy involves reducing the reflow peak temperature, shifting from ~245°C (typical for SAC alloys) to < 180°C using low-temperature Sn–Bi–based solder balls. However, when combined with SAC pastes, careful attention must be paid to the interfacial behavior between the two alloys. The mixing and solidification dynamics at the interface can lead to uneven microstructures, brittle intermetallic compounds (IMCs), and reliability concerns. Therefore, understanding and controlling the interaction between Sn–Bi balls and SAC pastes during reflow remains a central challenge for developing robust, low-temperature soldering solutions. During reflow, the Sn–Bi solder balls (melting at around 138°C) liquefy first, whereas the SAC paste, with a higher melting point (217°C–221°C), may remain solid or only partially melt depending on the thermal profile. This leads to asymmetric and sequential solidification, in which the molten Sn–Bi can infiltrate the SAC region,

29401402, 0, Downloaded from https://onlinelibrary.wiley.com/doi/10.1002/metm.70015 by Capes, Wiley Online Library on [13/10/2025]. See the Terms and Conditions (https://onlinelibrary.wiley.com/terms-and-conditions) on Wiley Online Library for rules of use; OA articles are governed by the applicable Creative Commons License

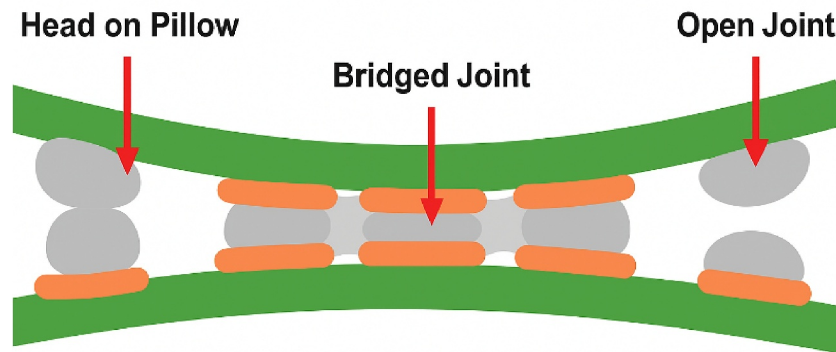

FIGURE 6 | Illustration of substrate warpage driven during reflow. Adopting low-temperature solders (reflow < 190°C) helps minimize this thermal distortion (unpublished image).

initiate early intermetallic diffusion, and alter the local composition. Upon cooling, solidification progresses unevenly, often resulting in Bi-rich segregation, uncontrolled growth of brittle IMCs like Ag_3Sn and Cu_6Sn_5, and heterogeneous eutectic structures at the interface. These phenomena can create localized porosity, sharp compositional gradients, and weak bonding zones, making solidification dynamics a key factor in the mechanical and thermal performance of hybrid solder joints.
An additional strategy involves introducing microalloying elements to achieve microstructural refinement. For instance, microadditions of antimony (Sb) to eutectic Sn–Bi solder alloys have been shown to have potential to reduce warpage by refining the microstructure and enhancing its thermal–mechanical stability [3]. Additionally, between 0.5 and 1 wt%, Sb may allow the formation of finely dispersed Sn–Sb intermetallic compounds, while inhibiting the growth of brittle Bi-rich lamellae. This refined microstructure improves ductility and reduces localized stress accumulation during solidification. As a result, the solder can better accommodate thermal contraction without inducing severe deformation, leading to noticeably lower warpage in assembled electronic components than the unmodified eutectic Sn–Bi alloy.

ii. X-ray microtomography (XMT) has become a powerful nondestructive tool for visualizing and quantifying solder joint microstructure in three dimensions, offering critical insights beyond what traditional 2D microscopy can reveal. This capability is especially valuable for detecting reflow-induced voids and Bi segregations in Sn–Bi/SAC hybrid joints. Looking ahead, the synergy of XMT with in situ thermal cycling and digital volume correlation (DVC) offers a future path for observing real-time damage evolution, such as void growth, IMC coarsening, and crack nucleation, enabling researchers to directly link processing conditions (like reflow profiles) to microstructural reliability outcomes. In a specific study on Sn–Bi alloys, Luktuke et al. [75] used 4D synchrotron-based XMT to reconstruct and track the three-dimensional evolution of microstructures during the directional solidification of an Sn–57 wt.% Bi eutectic alloy. They visualized, in real time, the growth of Bi-rich pyramidal structures and documented the dynamic segregation of Bi as solidification progressed. Their observations revealed heterogeneous phase distribution and complex solid–liquid interface morphologies, providing key insights into how solidification dynamics influence the resulting microstructure.

iii. Nanoindentation is a critical tool for evaluating the mechanical behavior of Sn–Bi solder alloys at the microscale, where heterogeneous microstructures (composed of soft Sn-rich, hard Bi-rich, and other phases) require localized property measurements [76]. This technique enables precise quantification of hardness and elastic modulus in individual phases or eutectic regions, providing insights into how microstructural features such as Bi segregation, eutectic refinement, or intermetallic formation affect overall joint performance. It is especially valuable for correlating phase morphology with ductility and fracture behavior, as well as assessing the effects of minor alloying additions on local mechanical reinforcement. Looking ahead, nanoindentation is expected to play a central role in the development of next-generation Sn–Bi–based solder alloys. Advances such as high-temperature and in situ nanoindentation will allow researchers to simulate service conditions and study creep or fatigue-related degradation at the nanoscale. Integration with techniques like EBSD or 3D x-ray tomography will enable detailed structure–property mapping.

iv. Sn–Bi alloys have shown promising self-healing behavior through localized melting under compressive stress and moderate heating, enabled by their solid–liquid two-phase region above the eutectic point [77–79]. This mechanism can repair microcracks and extend joint life, especially when enhanced by In additions that improve ductility and reduce the melting point [47, 80]. However, ensure long-term reliability requires addressing microstructural stability, particularly Bi coarsening and IMC growth, issues that remain underexplored at elevated temperatures for Sn–Bi alloys. Prospectively, Sn–Bi and Sn–Bi–In alloys offer strong potential for semisolid processing and low-temperature additive manufacturing. Their eutectic nature supports controlled phase morphology and low-

29401402, 0, Downloaded from https://onlinelibrary.wiley.com/doi/10.1002/metm.70015 by Capes, Wiley Online Library on [13/10/2025]. See the Terms and Conditions (https://onlinelibrary.wiley.com/terms-and-conditions) on Wiley Online Library for rules of use; OA articles are governed by the applicable Creative Commons License

thermal-budget fabrication ideal for flexible electronics and fine-pitch assemblies. Future research should focus on alloy design, solidification control, coarsening resistance, and interface bonding.

Acknowledgments

The authors would like to express their gratitude and pay tribute to the legacy of Prof. Amauri Garcia from University of Campinas, Brazil, in the field of solder alloy development, including his contributions to the search for Sn–Bi alloys with improved properties and a deeper understanding of the underlying mechanisms. We extend him our deepest thanks.

Conflicts of Interest

The authors declare no conflicts of interest.

Data Availability Statement

The data that support the findings of this study are available from the corresponding author upon reasonable request.

References

1. G. Henshall, R. Healey, R. S. Pandher, K. Sweatman, K. Howell, and R. Coyle, "Addressing Opportunities and Risks of Pb-Free Solder Alloy Alternatives," in *2009 European Microelectronics & Packaging Conference* (2009), 1–11.

2. R. J. Coyle, K. Sweatman, and B. Arfaei, "Thermal Fatigue Evaluation of Pb-Free Solder Joints: Results, Lessons Learned, and Future Trends," *Journal of the Minerals Metals & Materials Society* 67 (2015): 2394–2415, https://doi.org/10.1007/s11837-015-1595-1.

3. S. A. Belyakov, R. J. Coyle, B. Arfaei, J. W. Xian, and C. M. Gourlay, "Microstructure and Damage Evolution During Thermal Cycling of Sn-Ag-Cu Solders Containing Antimony," *Journal of Electronic Materials* 50 (2021): 825–841, https://doi.org/10.1007/s11664-020-08507-x.

4. S. A. Belyakov, B. Arfaei, C. Johnson, K. Howell, R. Coyle, and C. M. Gourlay, "Phase Formation and Solid Solubility in High Reliability Pb-Free Solders Containing Bi, Sb or In," in *Proceedings of SMTA International* (2019), 492–506.

5. R. Coyle, M. Reid, C. Ryan, et al., "The Influence of the Pb-Free Solder Alloy Composition and Processing Parameters on Thermal Fatigue Performance of a Ceramic Chip Resistor," *Proceedings of Electronic Components and Technology Conference* (2009): 423–430, https://doi.org/10.1109/ECTC.2009.5074048.

6. T. Laurila, V. Vuorinen, and J. K. Kivilahti, "Interfacial Reactions Between Lead-Free Solders and Common Base Materials," *Materials Science and Engineering* 49 (2005): 1–60, https://doi.org/10.1016/j.mser.2005.03.001.

7. L. E. Felton, C. H. Raeder, and D. B. Knorr, "The Properties of Tin-Bismuth Alloy Solders," *Journal of the Minerals Metals & Materials Society* 45 (1993): 28–32, https://doi.org/10.1007/BF03222377.

8. K. Tu, "Copper–Tin Reactions in Bulk Samples," in *Solder Joint Technology, Springer Series in Materials Science* (2007), 37–71, https://doi.org/10.1007/978-0-387-38892-2_2.

9. H. Kang, S. H. Rajendran, and J. P. Jung, "Low Melting Temperature Sn-Bi Solder: Effect of Alloying and Nanoparticle Addition on the Microstructural, Thermal, Interfacial Bonding, and Mechanical Characteristics," *Metals (Basel)* 11 (2021): 364, https://doi.org/10.3390/met11020364.

10. M. Abtew and G. Selvaduray, "Lead-Free Solders in Microelectronics," *Materials Science and Engineering* 27 (2000): 95–141, https://doi.org/10.1016/S0927-796X(00)00010-3.

11. S. Choi, J. P. Lucas, K. N. Subramanian, and T. R. Bieler, "Formation and Growth of Interfacial Intermetallic Layers in Eutectic Sn-Ag Solder and Its Composite Solder Joints," *Journal of Materials Science: Materials in Electronics* 11 (2000): 497–502, https://doi.org/10.1023/A:1008968518512.

12. U.S. Geological Survey, *Mineral Commodity Summaries 2024*. US Department of the Interior (United States Geological Survey, 2024), https://doi.org/10.3133/mcs2024.

13. London Metal Exchange (LME), *Official Prices for Ag, Sn, and Cu–2024* (London Met. Exch, 2024), https://www.lme.com/en/Metals/Non-ferrous.

14. N. Jiang, L. Zhang, Z. Liu, et al., "Reliability Issues of Lead-Free Solder Joints in Electronic Devices," *Science and Technology of Advanced Materials* 20 (2019): 876–901, https://doi.org/10.1080/14686996.2019.1640072.

15. A. I. M. Solder, "Low-Temperature Soldering: Challenges, Opportunities, and Considerations," (May 2025), https://www.aimsolder.com/blog/low-temperature-soldering-challenges-opportunities-and-considerations/.

16. L. Zhang, J. Han, C. He, and Y. Guo, "Reliability Behavior of Lead-Free Solder Joints in Electronic Components," *Journal of Materials Science: Materials in Electronics* 24 (2013): 172–190, https://doi.org/10.1007/s10854-012-0720-y.

17. C. D. S. Simioli, G. L. De Gouveia, and J. E. Spinelli, "Assessing the Microstructure of Sn—Bi—Zn Alloys During Semisolid Treatment," *Advanced Engineering Materials* 25 (2025): 2500325, https://doi.org/10.1002/adem.202500325.

18. S. A. Belyakov and C. M. Gourlay, "Intermetallics NiSn4 Formation During the Solidification of Sn e Ni Alloys," *Intermetallics* 25 (2012): 48–59, https://doi.org/10.1016/j.intermet.2012.02.010.

19. O. Gusakova, V. Shepelevich, and L. Scherbachenko, "Effect of Melt Cooling Rate on Microstructure of Sn–Bi and Sn–Pb Eutectic Alloys," *Advanced Materials Research* 856 (2014): 236–240, https://doi.org/10.4028/www.scientific.net/AMR.856.236.

20. Z. Chen, J. Zhang, S. Wang, and C. Wong, "Challenges and Prospects for Advanced Packaging," *Fundamental Research* 4 (2024): 1455–1458, https://doi.org/10.1016/j.fmre.2023.04.014.

21. X. F. Tan, Q. Hao, J. Zhou, S. D. McDonald, K. Sweatman, and K. Nogita, "Temperature-Dependent Electrical Resistivity in Sn-Bi Alloys," in *2024 International Conference on Electronic Packaging Technology* (2024), 207–208, https://doi.org/10.23919/ICEP61562.2024.10535619.

22. K. J. Puttlitz, "Overview of Lead-Free Solder Issues Including Selection," in *Handbook of Lead-Free Solder Technology* (Microelectronic Assembly, 2004), 48.

23. A. A. El-Daly and A. E. Hammad, "Development of High Strength Sn–0. 7Cu Solders With the Addition of Small Amount of Ag and In," *Journal of Alloys and Compounds* 509 (2011): 8554–8560, https://doi.org/10.1016/j.jallcom.2011.05.119.

24. D. Li, C. Liu, and P. P. Conway, "Characteristics of Intermetallics and Micromechanical Properties During Thermal Ageing of Sn–Ag–Cu Flip-Chip Solder Interconnects," *Materials Science and Engineering A* 391 (2005): 95–103, https://doi.org/10.1016/j.msea.2004.10.007.

25. D. R. Frear, J. W. Jang, J. K. Lin, and C. Zhang, "Pb-Free Solders for Flip-Chip Interconnects," *Journal of the Minerals Metals & Materials Society* 53 (2001): 28–33, https://doi.org/10.1007/s11837-001-0099-3.

26. H. Ma and J. C. Suhling, "A Review of Mechanical Properties of Lead-Free Solders for Electronic Packaging," *Journal of Materials Science* 44 (2009): 1141–1158, https://doi.org/10.1007/s10853-008-3125-9.

29401402, 0, Downloaded from https://onlinelibrary.wiley.com/doi/10.1002/metm.70015 by Capes, Wiley Online Library on [13/10/2025]. See the Terms and Conditions (https://onlinelibrary.wiley.com/terms-and-conditions) on Wiley Online Library for rules of use; OA articles are governed by the applicable Creative Commons License

27. G. Wu, J. Shen, D. Zhou, M. K. Faiz, and Y. H. Wong, "Applications and Recent Advances of Low-Temperature Multicomponent Solders in Electronic Packaging: A Review," *Micromachines* 16 (2025): 300, https://doi.org/10.3390/mi16030300.

28. T. T. Dele-afolabi, M. N. M. Ansari, and M. A. A. Hanim, "Recent Advances in Sn-Based Lead-free Solder Interconnects for Microelectronics Packaging: Materials and Technologies," *Journal of Materials Research and Technology* 25 (2023): 4231–4263, https://doi.org/10.1016/j.jmrt.2023.06.193.

29. W. Kurz, *F. D. J., Fundamentals of Solidification*, 4th ed. (Trans Tech Publications Ltd, 2005).

30. G. L. F. Powell and G. A. Colligan, "Solidification of Undercooled Sn-Bi and Pb-Sb Alloys," *Metallurgical Transactions A* 1 (1970): 133–138, https://doi.org/10.1007/BF02819252.

31. M. F. X. Gigliotti, G. L. Powell, and G. Colligan, "A Temperature-Composition Zone of Coupled Eutectic Growth in the Sn-Bi System," *Metallurgical Transactions A* 1 (1970): 1038–1041, https://doi.org/10.1007/bf02811795.

32. A. Kofler, "Precipitation Anomalies During Isothermal Crystallization From Undercooled, Binary Organic Melts," *Journal of the Australian Institute of Metals* 10 (1965): 132–139.

33. G. A. Chadwick, "Controlled Eutectic Growth," in *Solidification of Metals, Iron and Steel Institute Publication*, Vol. 110 (1968), 138–148.

34. T. Nishimura, "Low-Temperature Solder Composition," US4816219A (1989), https://patents.google.com/patent/US4816219A/en.

35. U. Kang, Y. Kwon, J. Lee, and C. Lee, "Tin-Bismuth (Sn-Bi) Family Alloy Solder and Semiconductor Device Using the Same," US20070152331A1 (2007), https://patents.google.com/patent/US20070152331A1/en.

36. M. Ueshima, Y. Inagawa, and M. Toyoda, "Bi—Sn Based High-Temperature Solder Alloy," US9205513B2 (2015), https://patents.google.com/patent/US9205513B2/en.

37. D. Werkhoven, A. Peeters, R. Lauwaert, I. Maris, B. Van De Lisdonk, and S. Teliszewski, "Lead-Free Solder Alloy Comprising Sn, Bi and at Least One of Mn, Sb, Cu and Its Use for Soldering an Electronic Component to a Substrate," WO2018046763A1 (2018), https://patents.google.com/patent/WO2018046763A1/en.

38. S. Zhang, H. He, X. Liu, et al., "SnBiSb Series Low-Temperature Lead-Free Solder and Its Preparation Method," US11479835B2 (2022), https://patents.google.com/patent/US11479835B2/en.

39. M. Maalekian and K. Seelig, "Lead-Free High Reliability Solder Alloys," US20170066089A1 (2017), https://patents.google.com/patent/US20170066089A1/en.

40. S. G. Gonya, J. K. Lake, R. C. Long, and R. N. Wild, "Lead-Free, Tin, Antimony, Bismtuh, Copper Solder Alloy," US 5411703A (1995), https://patents.google.com/patent/US5411703A/en.

41. R. Pandher, B. Singh, S. Sarkar, et al., "High Impact Toughness Solder Alloy," EP 2739432B1 (2022), https://data.epo.org/publication-server/rest/v1.0/publication-dates/20220105/patents/EP2739432NWB1/document.pdf.

42. F. M. Mutuku, N.-C. Lee, and H. Zhang, "SnBi and SnIn Solder Alloys," US11999018B2 (2024), https://patents.google.com/patent/US11999018B2/en.

43. L. Shen, P. Septiwerdani, and Z. Chen, "Elastic Modulus, Hardness and Creep Performance of SnBi Alloys Using Nanoindentation," *Materials Science and Engineering A* 558 (2012): 253–258, https://doi.org/10.1016/j.msea.2012.07.120.

44. W. Zhu, W. Zhang, W. Zhou, and P. Wu, "Improved Microstructure and Mechanical Properties for SnBi Solder Alloy by Addition of Cr Powders," *Journal of Alloys and Compounds* 789 (2019): 805–813, https://doi.org/10.1016/j.jallcom.2019.03.027.

45. Y. Goh, A. S. M. A. Haseeb, M. Faizul, and M. Sabri, "Effects of Hydroquinone and Gelatin on the Electrodeposition of Sn–Bi Low Temperature Pb-Free Solder," *Electrochimica Acta* 90 (2013): 265–273, https://doi.org/10.1016/j.electacta.2012.12.036.

46. F. Hua, Z. Mei, and J. Glazer, "Eutectic Sn-Bi as an Alternative to Pb-Free Solders," in *48th Electronic Components and Technology Conference* (1998), 277–283.

47. Q. I. N. Li, N. Ma, Y. Lei, J. Lin, H. Fu, and J. Gu, "Characterization of Low-Melting-Point Sn-Bi-In Lead-Free Solders," *Journal of Electronic Materials* 45 (2016): 5800–5810, https://doi.org/10.1007/s11664-016-4366-z.

48. B. L. Silva, G. Reinhart, H. Nguyen-thi, N. Mangelinck-noël, A. Garcia, and J. E. Spinelli, "Microstructural Development and Mechanical Properties of a Near-Eutectic Directionally Solidified Sn–Bi Solder Alloy," *Materials Characterization* 107 (2015): 43–53, https://doi.org/10.1016/j.matchar.2015.06.026.

49. B. L. Silva, V. C. E. da Silva, A. Garcia, and J. E. Spinelli, "Effects of Solidification Thermal Parameters on Microstructure and Mechanical Properties of Sn-Bi Solder Alloys," *Journal of Electronic Materials* 46 (2017): 1754–1769, https://doi.org/10.1007/s11664-016-5225-7.

50. W. R. Osório, L. C. Peixoto, L. R. Garcia, N. Mangelinck-noël, and A. Garcia, "Microstructure and Mechanical Properties of Sn–Bi, Sn–Ag and Sn–Zn Lead-Free Solder Alloys," *Journal of Alloys and Compounds* 572 (2013): 97–106, https://doi.org/10.1016/j.jallcom.2013.03.234.

51. R. Kakitani, C. A. P. da Silva, B. Silva, A. Garcia, N. Cheung, and J. E. Spinelli, "Local Solidification Thermal Parameters Affecting the Eutectic Extent in Sn-Cu and Sn-Bi Solder Alloys," *Soldering & Surface Mount Technology* 34 (2022): 24–30.

52. A. Z. Miric and A. Grusd, "Lead-Free Solders," *Soldering & Surface Mount Technology* 10 (1998): 18–25.

53. R. S. Sidhu and N. Chawla, "Microstructure Characterization and Creep Behavior of Pb-Free Sn-Rich Solder Alloys: Part I," *Microstructure Characterization of Bulk Solder and Solder/Copper Joints* 39 (2008): 340–348, https://doi.org/10.1007/s11661-007-9414-0.

54. W. J. Tomlinson and A. Fullylove, "Strength of Tin-Based Soldered Joints," *Journal of Materials Science* 27 (1992): 5777–5782, https://doi.org/10.1007/BF01119737.

55. C. Melton, "The Effect of Reflow Process Variables on the Wettability of Lead-Free Solders," *Journal of the Minerals Metals & Materials Society* 45 (1993): 33–35, https://doi.org/10.1007/BF03222378.

56. E. Çadirli, M. Sahin, R. Kayali, M. Ari, and S. Durmus, "Dependence of Electrical and Thermal Conductivity on Temperature in Directionally Solidified Sn–3. 5 wt % Ag Eutectic Alloy," *Journal of Materials Science: Materials in Electronics* 22 (2011): 1709–1714, https://doi.org/10.1007/s10854-011-0350-9.

57. G. Ren and M. N. Collins, "Improved Reliability and Mechanical Performance of Ag Microalloyed Sn58Bi Solder Alloys," *Metals (Basel)* 9 (2019): 462, https://doi.org/10.3390/met9040462.

58. B. L. Silva, A. Garcia, and J. E. Spinelli, "Cooling Thermal Parameters and Microstructure Features of Directionally Solidified Ternary Sn–Bi–(Cu, Ag) Solder Alloys," *Materials Characterization* 114 (2016): 30–42, https://doi.org/10.1016/j.matchar.2016.02.002.

59. K. A. Jackson and J. D. Hunt, "Lamellar and Rod Eutectic Growth," *Transactions of the Metallurgical Society of AIME* 236 (1966): 1129–1141, https://doi.org/10.1016/B978-0-08-092523-3.50040-X.

60. B. L. Silva, M. G. C. Xavier, and J. E. Spinelli, "Cu and Ag Additions Affecting the Solidification Microstructure and Tensile Properties of Sn-Bi Lead-Free Solder Alloys," *Materials Science and Engineering A* 705 (2017): 325–334, https://doi.org/10.1016/j.msea.2017.08.059.

61. B. L. Silva, A. Garcia, and J. E. Spinelli, "Complex Eutectic Growth and Bi Precipitation in Ternary Sn-Bi-Cu and Sn-Bi-Ag Alloys," *Journal*

29401402, 0, Downloaded from https://onlinelibrary.wiley.com/doi/10.1002/metm.70015 by Capes, Wiley Online Library on [13/10/2025]. See the Terms and Conditions (https://onlinelibrary.wiley.com/terms-and-conditions) on Wiley Online Library for rules of use; OA articles are governed by the applicable Creative Commons License

of Alloys and Compounds 691 (2016): 600–605, https://doi.org/10.1016/j.jallcom.2016.09.003.

62. K. M. Razeeb, E. Dalton, G. L. W. Cross, and A. J. Robinson, "Present and Future Thermal Interface Materials for Electronic Devices," *International Materials Reviews* 63 (2018): 1743–2804, https://doi.org/10.1080/09506608.2017.1296605.

63. K. C. Otiaba, N. N. Ekere, R. S. Bhatti, S. Mallik, M. O. Alam, and E. H. Amalu, "Thermal Interface Materials for Automotive Electronic Control Unit: Trends, Technology and R & D Challenges," *Microelectronics Reliability* 51 (2011): 2031–2043, https://doi.org/10.1016/j.microrel.2011.05.001.

64. J. Due and A. J. Robinson, "Reliability of Thermal Interface Materials: A Review," *Applied Thermal Engineering* 50 (2013): 455–463, https://doi.org/10.1016/j.applthermaleng.2012.06.013.

65. V. C. E. da Silva, G. L. de Gouveia, R. A. V. Reyes, A. Garcia, and J. E. Spinelli, "Sn-Bi (-Ga) TIM Alloys: Microstructure, Tensile Properties, Wettability and Interfacial Reactions," *Journal of Electronic Materials* 48 (2019): 4773–4788, https://doi.org/10.1007/s11664-019-07286-4.

66. R. Prasad, Surface Mount Technology: Principles and Practice (2013).

67. N. Eustathopoulos, "Wetting by Liquid Metals—Application in Materials Processing: The Contribution of the Grenoble Group," *Metals (Basel)* 5 (2015): 350–370, https://doi.org/10.3390/met5010350.

68. F. Wang, H. Chen, Y. Huang, L. Liu, and Z. Zhang, "Recent Progress on the Development of Sn–Bi Based Low-Temperature Pb-Free Solders," *Journal of Materials Science: Materials in Electronics* 30 (2019): 3222–3243, https://doi.org/10.1007/s10854-019-00701-w.

69. B. L. Silva, A. Garcia, and J. E. Spinelli, "Wetting Behavior of Sn–Ag–Cu and Sn–Bi–X Alloys: Insights Into Factors Affecting Cooling Rate," *Journal of Materials Research and Technology* 8 (2019): 1581–1586, https://doi.org/10.1016/j.jmrt.2018.06.016.

70. J. R. da S. Leal, R. A. V. Reyes, G. L. de Gouveia, F. G. Coury, and J. E. Spinelli, "Evaluation of Solidification and Interfacial Reaction of Sn-Bi and Sn-Bi-In Solder Alloys in Copper and Nickel Interfaces," *Metals (Basel)* 14 (2024): 963, https://doi.org/10.3390/met14090963.

71. A. Nabihah and M. S. Nurulakmal, "Effect of In Addition on Microstructure, Wettability and Strength of SnCu Solder," *Materials Today: Proceedings* 17 (2019): 803–809, https://doi.org/10.1016/j.matpr.2019.06.366.

72. C. Lo, T. Chang, T. Lee, and S. Hwang, "Analysis of Warpage and Reliability of Very Thin Profile Fine Pitch Ball Grid Array," *Heliyon* 10 (2024): e35459, https://doi.org/10.1016/j.heliyon.2024.e35459.

73. M. Abdel, M. Meilunas, X. A. Cao, J. Wilcox, and A. Ramini, "Effects of Solder Solidification Temperature on Residual Stress Distribution and Failure Location in BGA Solder Joints," *Microelectronics Reliability* 166 (2025): 115609, https://doi.org/10.1016/j.microrel.2025.115609.

74. P. Praful and C. Bailey, "Warpage in Wafer-Level Packaging: A Review of Causes, Modelling, and Mitigation Strategies," *Frontiers in Electronics* 5 (2025): 1515860, https://doi.org/10.3389/felec.2024.1515860.

75. A. Luktuke, A. L. Kastengren, V. Nikitin, H. Torbati-Sarraf, and N. Chawla, "Bismuth Pyramid Formation During Solidi fi Cation of Eutectic Tin-Bismuth Alloy Using 4D X-Ray Microtomography," *Communications Materials* 5 (2024): 95, https://doi.org/10.1038/s43246-024-00538-9.

76. X. F. Tan, V. Paul, T. Ohmura, S. D. McDonald, and K. Nogita, "Nanoindentation Study of Phases in Near-Eutectic Sn-Bi Alloy," in *2025 International Conference on Electronics Packaging and iMAPS All Asia Conference* (2025), 79–80, https://doi.org/10.23919/ICEP-IAAC64884.2025.11002920.

77. G. Siroky, E. Kraker, J. Rosc, et al., "Analysis of Sn-Bi Solders: X-Ray Micro Computed Tomography Imaging and Microstructure Characterization in Relation to Properties and Liquid Phase Healing Potential," *Materials (Basel)* 14 (2021): 153.

78. C. R. Fisher, H. B. Henderson, M. S. Kesler, et al., "Repairing Large Cracks and Reversing Fatigue Damage in Structural Metals," *Applied Materials Today* 13 (2018): 64–68, https://doi.org/10.1016/j.apmt.2018.07.003.

79. G. Siroky, E. Kraker, J. Magnien, et al., "Effect of Solder Joint Size and Composition on Liquid-Assisted Healing," *Microelectronics Reliability* 119 (2021): 114066, https://doi.org/10.1016/j.microrel.2021.114066.

80. Y. Liu and K. N. Tu, "Low Melting Point Solders Based on Sn, Bi, and In Elements," *Materials Today Advances* 8 (2020): 100115, https://doi.org/10.1016/j.mtadv.2020.100115.

29401402, 0, Downloaded from https://onlinelibrary.wiley.com/doi/10.1002/metm.70015 by Capes, Wiley Online Library on [13/10/2025]. See the Terms and Conditions (https://onlinelibrary.wiley.com/terms-and-conditions) on Wiley Online Library for rules of use; OA articles are governed by the applicable Creative Commons License